Available online at www.sciencedirect.com
SCIENCE DIRECT
Polymer 47 (2006) 3325–3335
polymer
www.elsevier.com/locate/polymer

Mechanistic investigation of 9-bromoanthracene photodimers as initiators in atom transfer radical polymerization

Amanda C. Roof, Eric S. Tillman *, Raleigh E. Malik, Alissa M. Roland, Daniel J. Miller, Louis R. Sarry

Department of Chemistry, Bucknell University, Lewisburg, PA 17837, USA

Received 9 August 2005; received in revised form 22 February 2006; accepted 8 March 2006
Available online 11 April 2006

Abstract

Mechanistic pathways accounting for the lack of control in polymerizations employing photodimers of 9-bromoanthracene as alkyl halide initiators in atom transfer radical polymerization (ATRP) reactions are presented. Converting the aryl bromide on the anthracene moiety into an alkyl bromide via a [4+4] cycloaddition reaction effectively generated the photodimer with two alkyl halide sites, which were investigated as potential initiating sites for the ATRP of styrene and *n*-butyl acrylate. Polymers synthesized using these photodimers as initiators possessed relatively broad polydispersity index (PDI) values and displayed a non-linear relationship between their number average molecular weights (M_n) and monomer consumption, consistent with slow initiation from the bridgehead alkyl halide. Reactions performed at 80 °C in bulk or THF generated polystyrene with M_n values 3–5 times higher than calculated based on monomer-to-initiator ratios. UV–vis spectrometry of the products demonstrated absorbance bands indicative of polymer-bound anthracene, caused by thermal degradation of the photodimer during the polymerization. When the initiator was introduced last into the reaction mixture in an attempt to suppress photodimer cleavage prior to initiation, PDI values and M_n values were generally lowered with the resulting polymers showing similarly high anthracene content. Composition of polystyrene and poly(*n*-butyl acrylate) products was also studied as a function of reaction temperature, with decreased anthracene labeling observed at lower temperatures (40 and 60 °C), further validating a model of heat-induced cleavage of the photodimer.

Keywords: Atom transfer radical polymerization; Polystyrene; Anthracene

1. Introduction

Atom transfer radical polymerization (ATRP) has successfully led to the controlled/living polymerization of vinyl monomers over a wide range of reaction conditions [1–5]. The key components essential for ATRP are the initiator species (R–X), the vinyl monomer (CH_2=CHR′), and a transition metal catalyst such as copper(I) halide complexed with a ligand (commonly a di- or tri-amine), as shown in Scheme 1. The position of the equilibrium heavily favors the more stable alkyl halide, drastically reducing competing termination pathways, most commonly radical combination or disproportionation, and allows the polymerization to proceed in a living fashion [2,6,7]. The transfer of the halogen atom on the initiator to the metal catalyst requires a suitable initiator capable of homolytic cleavage of the C–X bond. ATRP reactions generally employ an alkyl halide (R–X) initiator, where X = Cl or Br and is bound to an sp^3 hybridized carbon [8,9] located on the alpha-carbon to an aryl group or an ester, for initiation of styrenic or alkyl acrylate monomers, respectively [10–12].

The synthesis of polymers labeled with aromatic chromophores via ATRP thus requires either an aromatic chromophore inherently containing an sp^3 hybridized C–X bond, such as 9-bromofluorene [13], or chemical modification of the aryl species to incorporate a suitable alkyl halide substituent capable of initiation [14–16]. This requirement may add several synthetic steps to the experimental procedure and often introduces functional groups, for example ester linkages between the chromophore and polymer chain [17,18], that may interfere with photophysical studies. Although the incorporation of aromatic chromophores into vinyl polymeric chains has been accomplished by anionic techniques involving nucleophilic coupling reactions, such as polystyryllithium with (halomethyl)anthracenes, side reactions typically lead to only partial chromophore labeling [19–22]. Additionally, the experimental leniency of radical polymerization, compared to

* Corresponding author. Tel.: +1 570 577 3265; fax: +1 570 577 1739.
E-mail address: etillman@bucknell.edu (E.S. Tillman).

0032-3861/$ - see front matter © 2006 Elsevier Ltd. All rights reserved.
doi:10.1016/j.polymer.2006.03.028

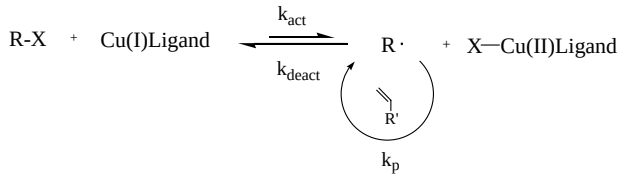

Scheme 1. General reaction scheme for ATRP employing alkyl halides as initiators.

anionic techniques, makes chromophore labeling methods that employ ATRP attractive. Ideally, direct polymerization from the aryl species could lead to chromophoric labels directly bound to the polymer, however, aryl halide initiators in ATRP have not been reported, presumably due to the inability of an sp^2 hybridized, aromatic C–X bond to undergo homolytic cleavage under ATRP conditions. Complications such as copper-catalyzed Ullmann–Goldberg coupling or analogous crosscoupling reactions [23–26] may further prevent the use of aryl halides in ATRP systems.

A reversible photodimerization of anthracene and substituted anthracene derivatives is known to occur through the 9-, 10- positions in a head to tail fashion at wavelengths longer than 300 nm, as shown in Scheme 2 [27–29]. If 9-bromoanthracene (a) is chosen, conversion of two aryl halides into alkyl halides, possibly suitable for use as initiators in ATRP, is accomplished. The facile thermolysis of the anthracene photodimer [21,27] would generate two polymer chains directly bound to the anthracene chromophore (Scheme 3).

In this paper, 9-bromoanthracene photodimers are studied as initiators in the ATRP of styrene and *n*-butyl acrylate. The mechanistic pathways responsible for slow initiation, degradation of the photodimer, and high amounts of anthracene labeling in the resulting polymers are presented.

2. Experimental

2.1. Materials

9-Bromoanthracene (94%, Aldrich) was recrystallized from ethanol and stored in the dark at room temperature. CuBr (98%, Aldrich) and CuCl (99.995+%, Aldrich) were used as received and stored in a desiccator at room temperature. Styrene (99%, Acros), *n*-butyl acrylate (99+%, Aldrich), *N,N,N′,N″,N″*-pentamethyldiethylenetriamine (PMDETA, 99%, Aldrich), and anisole (99.7%, Aldrich) were distilled from calcium hydride under reduced pressure and stored in sealed glass

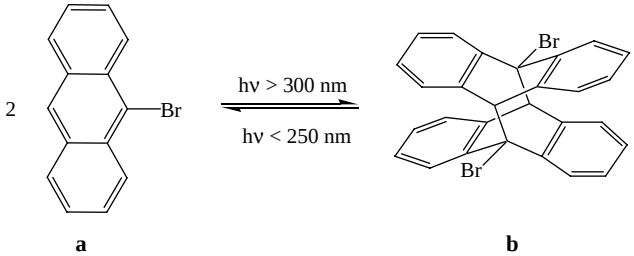

Scheme 2. Reversible photodimerization of 9-bromoanthracene (a) to generate the photodimer (b).

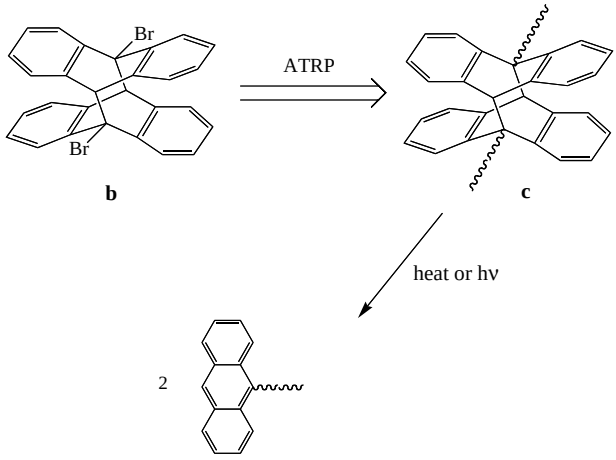

Scheme 3. Condensed synthetic plan for the ATRP of styrene using photodimers of 9-bromoanthracene as initiators, leading to anthracene end-labeled polystyrene (d).

ampoules at −15 °C. 1-Bromonaphthalene (97%, Aldrich) was used as received. Tetrahydrofuran (THF) was distilled from sodium/benzophenone prior to use. Benzene was passed through a Grubbs-type purification column [30] before use.

2.2. Typical photodimerization of 9-bromoanthracene (synthesis of 9,9′-dibromodianthracene)

2.0 g (7.78 mmol) of 9-bromoanthracene was dissolved in 65 mL of benzene. The flask was equipped with a condensing column and drying tube, and irradiated with longwave UV light (Blak-Ray; Model B100 AP, $\lambda = 365$ nm). The photodimerization was monitored using UV–vis spectroscopy and was considered complete when the absorption peaks due to anthracene (between 350 and 400 nm, max at 370 nm) completely disappeared (~48 h). The volatiles were removed under vacuum and the residue was washed with cold benzene to afford the title compound as a yellowish-white solid. The photodimer was characterized by UV–vis spectroscopy, ^{1}H NMR, and melting point (Mp = 200–202 °C). ^{1}H NMR ($CDCl_3$): δ (ppm) 7.77 (d, 8H, $J = 8.52$ Hz), 6.95 (m, 8H), 5.33 (s, 2H).

2.3. Typical ATRP procedure using the photodimer of 9-bromoanthracene as the initiator. ($[M]_0:[I]_0 = 50:1$; $[Cu(I)]_0:[I]_0 = 2.5:1$; $[Cu]_0$–$[PMDETA]_0$)

The reaction parameters were calculated based on monomer to initiating-sites ratio ([I] = [C–Br]), usually keeping the monomer volume constant (~2.0 mL) and ratio of Cu(I)X (X = Br, Cl) to PMDETA at 1. 9-Bromoanthracene (89.5 mg, 0.174 mmol) photodimer initiator and 124.8 mg CuBr (0.870 mmol) were placed in a two-necked round bottom flask, after which one neck was sealed with a septa and the other with a Teflon stop cock. After being placed on a Schlenk line and filled with nitrogen gas, sequential additions of 2.0 mL styrene (17.4 mmol) and 2.1 mL THF (~50% by volume) were introduced into the flask via argon purged syringes

followed by a total of three freeze–pump–thaw cycles. If the reaction was performed in the dark, the entire flask was covered in aluminum prior to the addition of solvent and monomer and remained covered for the duration of the reaction. The reaction chamber was sealed, removed from the line, and placed in an oil bath preheated to 80 °C. After allowing the contents of the flask to reach the temperature of the oil bath, 0.182 mL (0.870 mmol) PMDETA was added through an argon-flushed syringe. After 48 h, the vessel was removed from the oil bath and the reaction mixture was dissolved in THF. The polymer was precipitated in cold methanol at least two times and dried in a vacuum oven (~45 °C) prior to characterization. Reactions employing *n*-butyl acrylate as the monomer (Table 4) were performed in an identical manner as above, except GPC characterization was performed on the crude reaction mixture.

Reactions performed with the photodimer initiator introduced last (Table 2) were carried out in an analogous manner, with a THF slurry of the initiator added via an argon-flushed syringe to the reaction mixture that had reached 80 °C. The ligand was introduced prior to the freeze–pump–thaw cycles in these cases, and THF solvent was added along with the initiator.

2.4. Characterization

Analysis of the polymers was performed on a Waters gel permeation chromatography (GPC) system connected to a PC running Waters Breeze software. The system consists of a Waters 1515 isocratic pump, a Waters 717 auto sampler, two Pl-gel 5 mm Mixed C columns (Polymer Labs), a Waters 2487 dual wavelength detector and a Waters 2414 RI detector. The mobile phase was THF in all cases, and a 10 point calibration using polystyrene standards (Polymer Laboratories, Mp range: 5.0×10^2–3.05×10^6 Da) was used to obtain molecular weights and polydispersities based on the RI traces. Concurrently, the UV detector was set at 370 nm to visualize the distribution of anthracene in the product. Percent monomer conversion values were calculated based on data obtained with gas chromatography (GC) using anisole as the internal standard in the polymerization. A Hewlett Packard HP 6890 GC with HP Chemstation software with 1 μL injections in THF solvent was used. NMR was performed with a Bruker 300 MHz FT-NMR at room temperature. The UV–vis data was obtained on a Gentech TU-1901 double-beam UV–vis Spectrophotometer with THF as the solvent.

3. Results and discussion

3.1. Effect of experimental conditions

The two alkyl halide sites generated from the [4+4] photocyclization of 9-bromoanthracene (Scheme 2) were employed as initiators in the ATRP of styrene, as outlined in Scheme 3. Cleavage of the centrally located anthracene photodimer in the polymer backbone should subsequently lead to two equivalents of anthracene end-labeled polystyrene (Scheme 3, d). Initial reactions were carried out using the isolated photodimer as the ATRP initiator, Cu(I)Br as the catalyst, and PMDETA as the ligand in THF solutions at 80 °C in both the presence and absence of light. As shown in Table 1 (runs 1 and 2), when reactions were carried out in uncovered glassware (light trials) the number average molecular weight (M_n) values of the polymer obtained was 3 to 4-fold higher than anticipated based on monomer to initiating-site ratios and possessed a fairly high polydispersity index (PDI) value (>1.6). Typical GPC traces (both RI and UV) of polystyrene formed under these conditions are shown in Fig. 1, bottom. The UV detector was set at 370 nm, an absorbance maximum for anthracene, and its trace qualitatively indicated the polymers formed were labeled with the anthracene chromophore, as neither the photodimer nor polystyrene itself absorbs at this wavelength. Both the RI and UV traces show unsymmetrical peaks with low molecular weight tails.

Polymerizations were performed under identical conditions but in the dark, in an attempt to suppress photochemistry of the

Table 1
Results of the ATRP of styrene using photodimers of 9-bromoanthracene as the initiator

Run	[M]/[I][a]	[Cu]/[I][b]	Light or dark	$V_{Solvent}/V_{Total}$	Time (h)	M_n[c] (Da)	PDI M_w/M_n
1	25	2.5	L	0.5	72	13,020	1.75
2	50	2.5	L	0.5	48	21,490	1.68
3	25	1.25	D	0.5	48	20,950	1.60
4	50	1.25	D	0.5	48	25,310	1.54
5	25	1.25	D	0.75	76	15,170	1.47
6[d]	50	2.5	D	0.7	72	16,010	1.68
7	50	2.5	D	0.5	48	24,800	1.59
8	100	2.5	D	0.5	48	22,220	1.34
9[d]	50	2.5	D	0.7	72	18,230	1.61
	50	2.5	D	0.7	48	17,650	1.63
	50	2.5	D	0.7	24	17,190	1.38
	50	2.5	D	0.7	12	11,240	1.36
	50	2.5	D	0.7	6	8320	1.23
10[d]	50	2.5	L	0.7	72	21,050	1.54
	50	2.5	L	0.7	48	20,390	1.53
	50	2.5	L	0.7	24	17,950	1.41
	50	2.5	L	0.7	12	12,160	1.24
	50	2.5	L	0.7	6	8190	1.23
11[e]	50	2.5	L	0.5	72	23,700	1.67
12[e]	100	2.5	L	0.5	72	38,720	1.59
13[e]	100	2.5	D	0.5	72	38,890	1.55
14[e]	50	2.5	D	0.5	48	18,700	1.82
15[e]	50	2.5	D	Bulk	48	26,080	1.75
16[e]	50	2.5	D	Bulk	48	22,400	1.84
17[e]	50	1	L	0.5	48	31,630	1.63
18[e]	50	1	L	0.5	48	23,130	1.55
19[e]	50	1	L	0.5	72	43,830	1.46
20[f]	50	2.5	L	0.5	48	144,480	1.71

Reactions were run with PMDETA as the ligand and Cu(I)Br (or Cu(I)Cl, as indicated) as the catalyst at 80 °C. See Section 2 for details.

[a] Monomer (M) = styrene. Initiator (I) = anthracene photodimer. ([I] = [C–Br sites]).

[b] Catalyst (CuX) to initiating sites (C–Br) ratio. [CuBr]–[PMDETA].

[c] Apparent number average molecular weight compared to PS standards using RI detection.

[d] Anisole was used as an internal standard ($V_{solvent} = V_{THF} + V_{anislole}$).

[e] Cu(I)Cl was used as the catalyst.

[f] 1-Bromonaphthalene was used as the initiator.

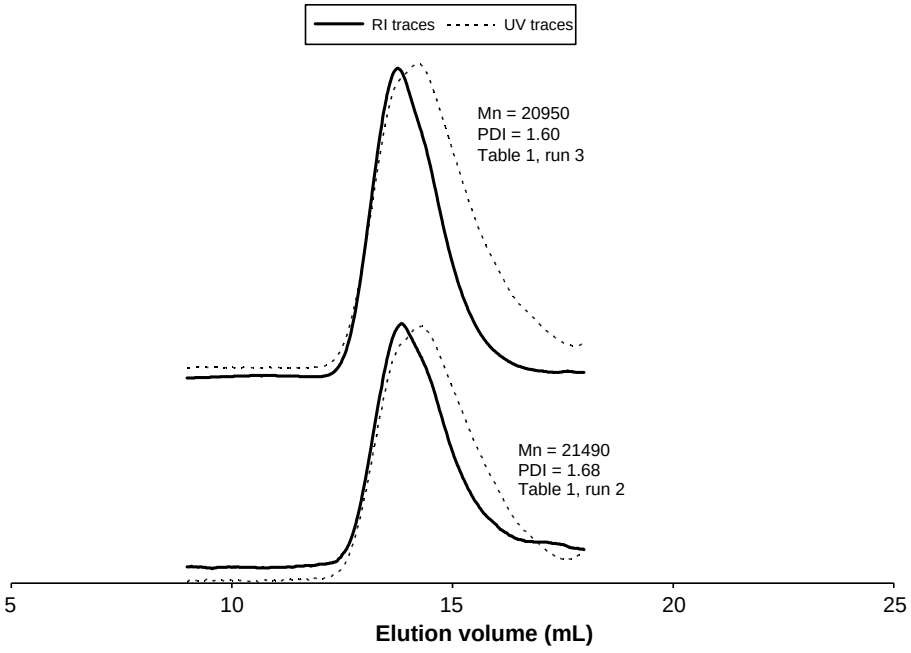

Fig. 1. GPC traces of anthracene-labeled polystyrene obtained by ATRP using photodimers of 9-bromoanthracene as the initiator, Cu(I)Br as the catalyst, and PMDETA as the ligand; performed in light (bottom) and the dark (top) (Table 1, runs 2 and 3, respectively). Solid line, RI trace; dashed line, UV trace (370 nm).

anthracene moiety that was found to be regenerated during the reaction. As seen in Table 1 (runs 3–8), polymers were formed with M_n values typically 3–4 times higher than calculated based on the ratio of monomer to initiating-sites, and with PDI values between ~1.4 and 1.7. Decreasing the ratio of [Cu(I)]:[PMDETA]:[C–Br sites] from 2.5:2.5:1 to 1.25:1.25:1 (runs 3–5) generally lead to polymers possessing lower PDI values. Typical GPC traces (RI and UV) of polystyrene generated with ATRP performed in the dark are shown in Fig. 1, top traces. The GPC-UV (370 nm) trace indicated the polymers formed were also labeled with anthracene (Scheme 3, d), rather than containing only the centrally bound photodimer (Scheme 3, c). Again, low molecular weight tails were observed on both RI and UV traces.

Both the M_n and PDI values of the propagating polymers were monitored over the course of two ATRP reactions (performed in both the light and the dark) and plotted as a function of monomer conversion (Fig. 2(a) and (b)). As shown in Fig. 2(a) (the light trial) the M_n values of the polymers slowly leveled near 40% monomer conversion, while the PDI values continued to rise throughout the polymerization. Also plotted are the calculated theoretical M_n values, based on either retention of the central photodimer in the polymer (Scheme 3, c; Fig. 2, solid line) or cleavage (Scheme 3, d; Fig. 2, dashed line), as a function of monomer consumption. Analogous experiments carried out in the dark displayed a flattening of M_n values near 40% monomer conversion and a continual rise in PDI values of the resulting polymers (Fig. 2(b)). In both cases, the observed M_n values were several-fold higher than calculated values at low monomer conversion and remained 3–4 times higher throughout the reaction.

Shown in Fig. 3 are kinetic plots, displaying $\ln([M]_0/[M]_t)$, where $[M]_0$ is the initial concentration of monomer and $[M]_t$ is the concentration of monomer at time t, as a function of reaction time, for the ATRP of styrene performed both in the light (○, dashed line) and the dark (♦, solid line). Both plots demonstrate the reaction to be first order with respect to monomer concentration and to be consuming monomer at a similar rate. The inset displays monomer conversion as a function of time for both experimental conditions, again showing no substantial differences for the two cases.

Fig. 4(a) and (b) shows the GPC traces (RI and UV detectors, respectively) of the propagating polymers at varying times throughout the ATRP reaction (performed in the dark; Table 1, run 9). The RI traces of the polymers show a low molecular weight tail, with an increase in M_n values throughout the course of the reaction that slows with increasing time (Fig. 4(a)). Similarly, the UV traces (set at 370 nm to visualize the anthracene-containing species) show a long, low molecular weight tail for each aliquot. Of note is the anthracene chromophore's presence in even the first sample, at $t=6$ h, indicating cleavage of the anthracene photodimer at early stages in the reaction. Analogous reactions performed in the presence of light (Table 1, run 10) showed no substantial differences to the traces displayed in Fig. 4(a) and (b).

By employing Cu(I)Cl as the catalyst instead of Cu(I)Br, the rate of polymerization is expected to be lowered by decreasing the k_{act}/k_{deact} ratio, where k_{act} is the rate of activation and k_{deact} is the rate of deactivation for the radical species, due to the increased strength of the C–Cl bond [31]. As shown in Table 1 (runs 11–19), polymers were produced with M_n values approximately 3–5 times higher than calculated, and PDI values ranging from 1.55 to 1.84. Again, no observable difference was found between runs performed in the presence or absence of light (runs 12 vs. 13). Performing reactions in bulk styrene generated polymers with similar PDI values as

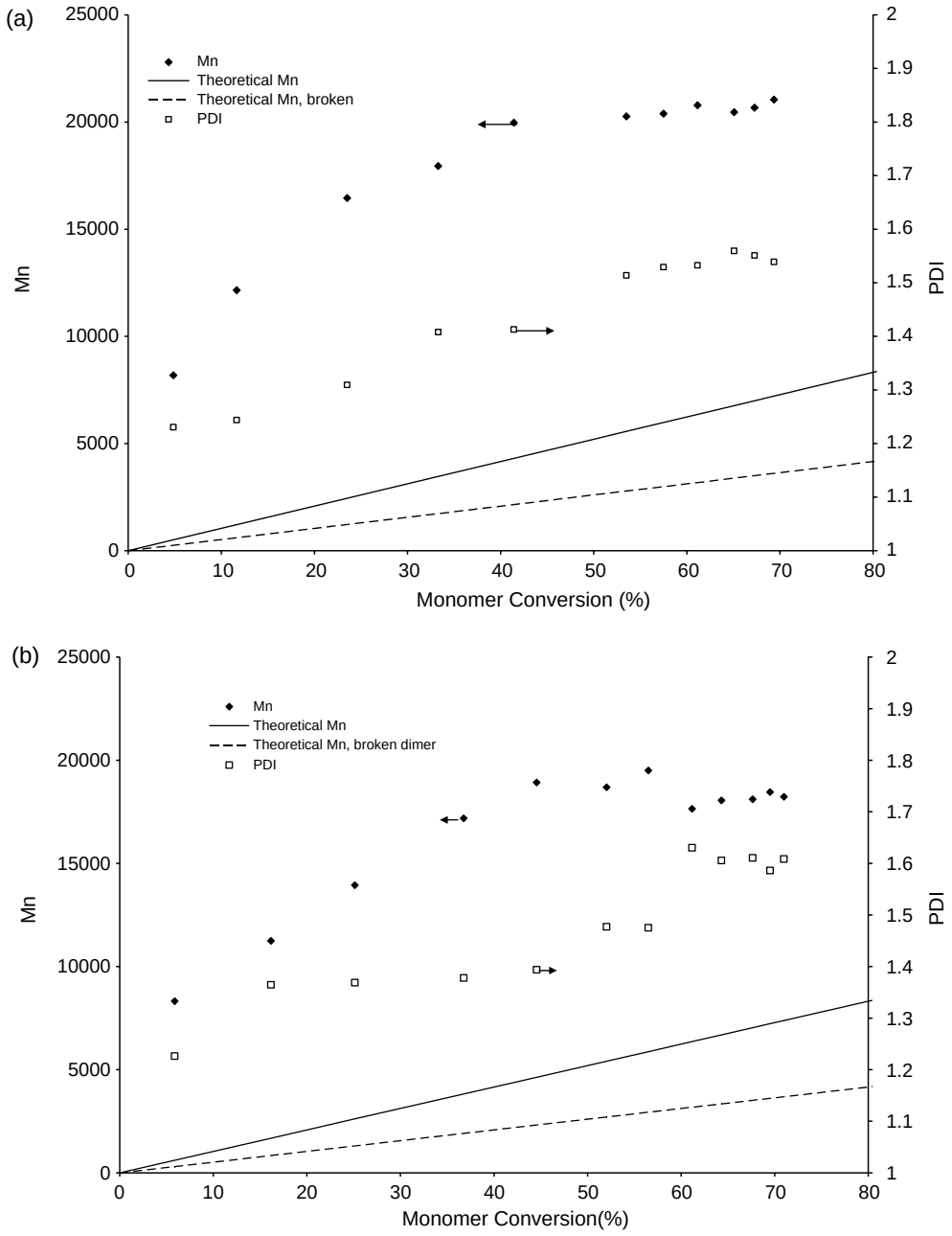

Fig. 2. Number average molecular weight (M_n) and PDI (M_w/M_n) vs. % monomer conversion for the ATRP of styrene using photodimers of 9-bromoanthracene as the initiator, Cu(I)Br as the catalyst, and PMDETA as the ligand at 80 °C in the light (a) and the dark (b). $[M]_0/[I]_0 = 50{:}1$. $[M]_0 = 2.92$ M; $[I]_0 = 0.058$ M; $[L]_0 - [Cu(I)]_0 = 0.0146$ M. Calculated M_n values as a function of % monomer conversion are plotted for polymers containing the centrally bound anthracene photodimer (solid line, Scheme 3, c) or end-labeled polymers (dashed line, Scheme 3, d).

those performed in THF (Table 1, runs 15–16). Decreasing the [Cu(I)]:[PMDETA]:[C–Br] ratio to 1:1:1 (runs 17–19) generally decreased the PDI of the resulting polymers (PDI < 1.63) compared to reactions performed using higher ratios (2.5:2.5:1).

3.2. ATRP with aryl halide initiators

To rule out the possibility that 9-bromoanthracene, or aryl halides in general, could act as ATRP initiators on their own, ATRP reactions were attempted using 1-bromonaphthalene as the initiator (Scheme 4; Table 1, run 20). This aryl halide was chosen due to expected similarities in reactivity compared to 9-bromoanthracene, yet its inability to photodimerize eliminates the possibility of small amounts of photodimer being present during initiation. While very high molecular weight polymer was formed during these reactions, analysis using UV–vis spectroscopy indicated the absence of aromatic chromophores on the polymer chain (naphthalene, in this case). Thus, the polystyrene was likely formed by heat-induced polymerization [32] consistent with the high M_n values, broad GPC traces, and lack of aromatic labeling. Thus, ATRP

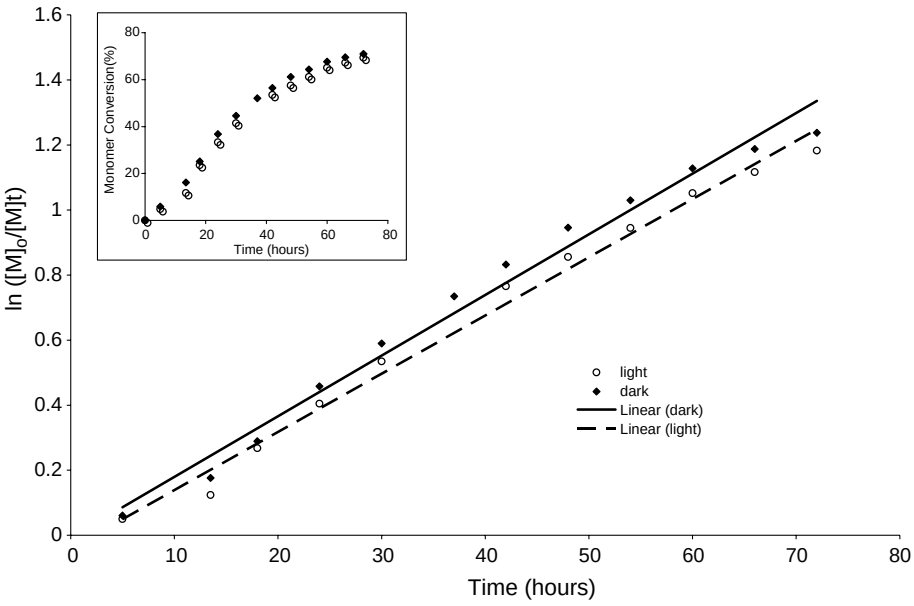

Fig. 3. First order kinetic plots for the ATRP of styrene using photodimers of 9-bromoanthracene as the initiator and PMDETA as the ligand at 80 °C; in the light (○, dashed line) and the dark (◆, solid line). $[M]_0/[I]_0 = 50{:}1$. $[M]_0 = 2.92$ M; $[I]_0 = 0.058$ M; $[L]_0$–$[Cu(I)]_0 = 0.146$ M. $[M]_0$ is the initial monomer concentration and $[M]_t$ is the monomer concentration at time t.

initiation directly from the aromatic C–Br bond on 9-bromoanthracene can be discounted.

3.3. Mechanistic account

The data presented above are consistent with a slow initiating system, further complicated by competing reactions occurring during the course of the polymerization resulting in polymers with fairly high PDI values and a non-linear relationship between M_n and monomer conversion. Thus, the uncontrolled nature of the system is not consistent with a typical ATRP system, which produces polymers in a highly controlled fashion. Thermolysis of the anthracene photodimer is occurring during the course of the reaction, generating polymers end-labeled with anthracene rather than containing the centrally-bound anthracene photodimer. Scheme 5 shows the possible pathways occurring during the reaction, which begins with the photodimer, b, as the only form of anthracene present. The photodimer can initiate a polymer chain, forming e, or may be cleaved prior to initiation, forming two equivalents of 9-bromoanthracene, a. Once formed, compound e may initiate another polymer arm from its remaining C–Br site, generating c, or it may be cleaved, creating 9-bromoanthracene and anthracene-labeled polymer, d. Because propagation occurs at the chain end, cleavage after initiation should not affect the controlled growth of the polymer [33,34]. If cleavage occurs before one or both initiating sites gives rise to a polymer chain, 9-bromoanthracene is formed, which is not able to initiate a chain (see discussion above). However, the reversibility of the cleavage of the photodimer may allow for the reformation of initiating sites during the course of the reaction, by cycloaddition of two 9-bromoanthracene species, a, or one 9-bromoanthracene with anthracene-labeled polymer, d, forming b or e, respectively. The possibility of pure thermal polymerization and transfer to the monomer could also contribute to the non-linearity of the plots of M_n as a function of monomer conversion, although at 80 °C these should be minimal in the case of styrene [32,35].

The fact that reactions performed in both the presence and absence of light showed no substantial differences, in either the polymer products nor kinetic analyses, indicate the pathways shown in Scheme 5 are not significantly affected by incidental laboratory light. The slightly lowered PDI values obtained for trials performed in the dark may suggest that re-formation of photodimers occurs to a slightly lowered degree than experiments performed in the presence of light.

Consider Scheme 6, which examines more closely the fate of a single initiating site (only one half of the photodimer is shown for clarity). The initial equilibrium (k_{act}/k_{deact}) between the dormant alkyl halide, A, and the radical, B, lies very far to the left, as the bridgehead radical is out of plane with the adjacent aromatic systems and thus unable gain appreciable resonance stabilization. The initiating radical, B, once formed may add across the double bond of styrene (k_{init}), forming C. The position of the equilibrium (k_{act}/k_{deact}) is responsible for the low concentration of B, and thus the slow rate of initiation (rate $= k_{init}[B]$) which presumably plays a large role in the non-linearity of M_n as a function of monomer conversion (Fig. 2). Once initiation occurs, the polymer will continue to propagate containing the photodimer intact, C, or cleaved, D, with the same propagation rate, as the k'_{act}/k'_{deact} ratio should depend only on the polystyrene chain end. The increased stability of the propagating radical, C or D, compared with the initiating radical, B, should lead to a larger value for $k'_{eq}(k'_{act}/k'_{deact})$ for the propagating species and thus a higher concentration of these radicals compared to initiating radicals.

The UV–vis spectra of the polymer products show characteristic anthracene absorptions, red-shifted from those

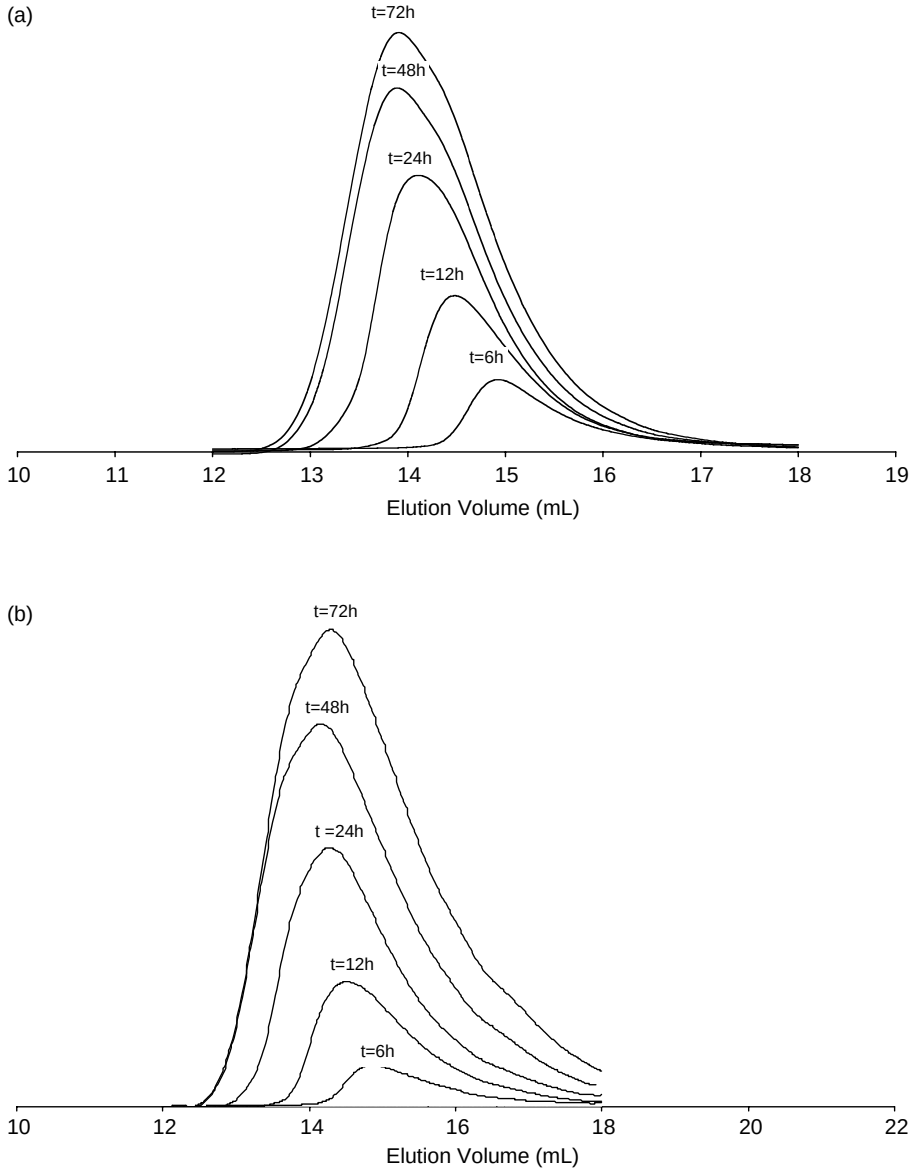

Fig. 4. GPC traces of polymers obtained using photodimers of 9-bromoanthracene in the dark as a function of time (Table 1, run 9). RI traces (a) and UV (370 nm) traces (b).

of molecular anthracene (Fig. 5), consistent with polymer-bound chromophores [16]. Substantial anthracene-labeling is observed in the polymer chains allowed to propagate ~48 h or longer (75 to ~100%), as calculated from Beer–Lambert's law [36]. Thus, during the course of the reaction, chains are initiated and cleaved, with nearly all chains cleaved by thermolysis of the photodimer by the end of the reaction period. Even the earliest polymer UV traces show absorbance at 370 nm (Fig. 4(b), at $t = 6$ h), indicating that cleavage is occurring at the beginning stages of the reaction. The inset of Fig. 5 shows the absorbance spectrum of 9-bromoanthracene (solid line), which is red-shifted by 2 nm compared to the polymer-bound anthracene, along with the initiating photodimer of 9-bromoanthracene, which shows no anthracene absorption.

From the data presented above, it can be determined that approximately 25% of the alkyl halide initiating sites give rise to polymer chains under the above conditions (Table 1, runs 9 and 10). This is arrived at based on the theoretical M_n of polymers with anthracene end groups (Fig. 2(a) and (b), dashed lines) compared to the experimentally observed values (~4 fold difference). Because the isolated polymers show high levels of anthracene labeling (Scheme 3, d) only small amounts

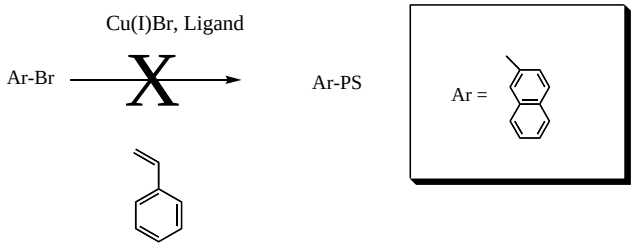

Scheme 4. ATRP using aryl bromides as initiators, giving no observable end-labeled polymers.

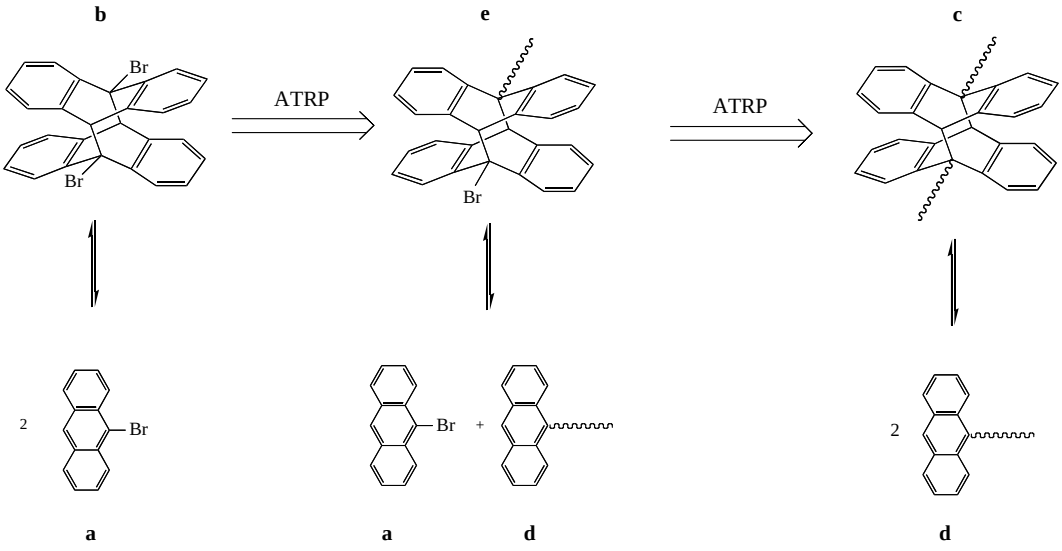

Scheme 5. Proposed reaction pathways occurring during the course of the ATRP reaction initiated with 9-bromoanthracene photodimers.

of product contained the centrally bound photodimer intact (Scheme 5, c). Thus, ∼6% of the initiating photodimers are expected to grow polymer chains off both C–Br initiating sites if each site has a 25% chance of initiation. Following through with this logic, most photodimers are cleaved prior to initiation, ∼55% (Scheme 5, b→a), while about ∼40% initiate a single chain before being cleaved (Scheme 5, e→d).

In an attempt to prevent the inadvertent cleavage of the 9-bromoanthracene photodimers prior to initiation, the addition order of the reactants was altered. Adding the photodimer last, after all other reagents have been introduced and allowed to reach reaction temperature, should reduce initiator decomposition and other side reactions prior to the beginning of the ATRP. As shown in Table 2, polymers produced using this method typically possessed lower PDI values (1.3–1.53) and had M_n values closer than anticipated (∼2–3-fold higher) compared to reactions where the ligand was added last (Table 1, runs 11–19 for comparison). Analysis of the polymers again showed absorbance bands indicative of polymer-bound anthracene, and calculations using Beer–Lambert's law demonstrated similarly high levels of anthracene labeling. This is consistent with the previously introduced model of heat-induced cleavage, with the initial decomposition decreased (Scheme 5, b→a) and cleavage occurring largely after initiation (Scheme 5, e→a+d; c→d).

3.4. Effect of temperature

To further evaluate the validity of the heat-induced cleavage model outlined in Schemes 5 and 6, polymerizations using styrene were performed at temperatures ranging from 80 °C down to 40 °C (Table 3). It is expected that at lower

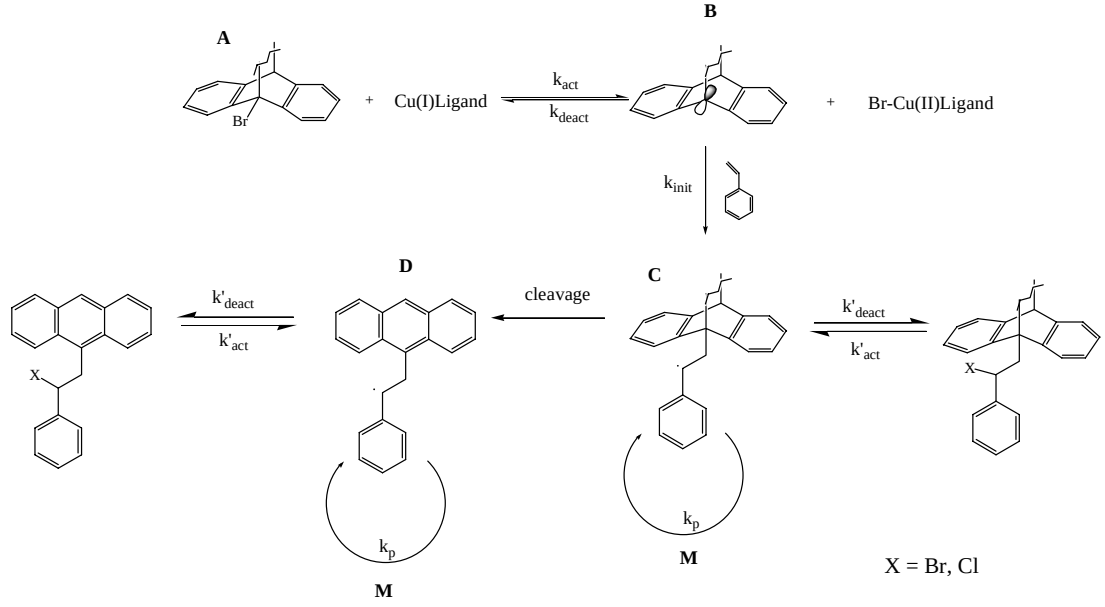

Scheme 6. Activation of one C–Br site on the photodimer of 9-bromoanthracene followed by initiation of polystyrene and cleavage of the photodimer.

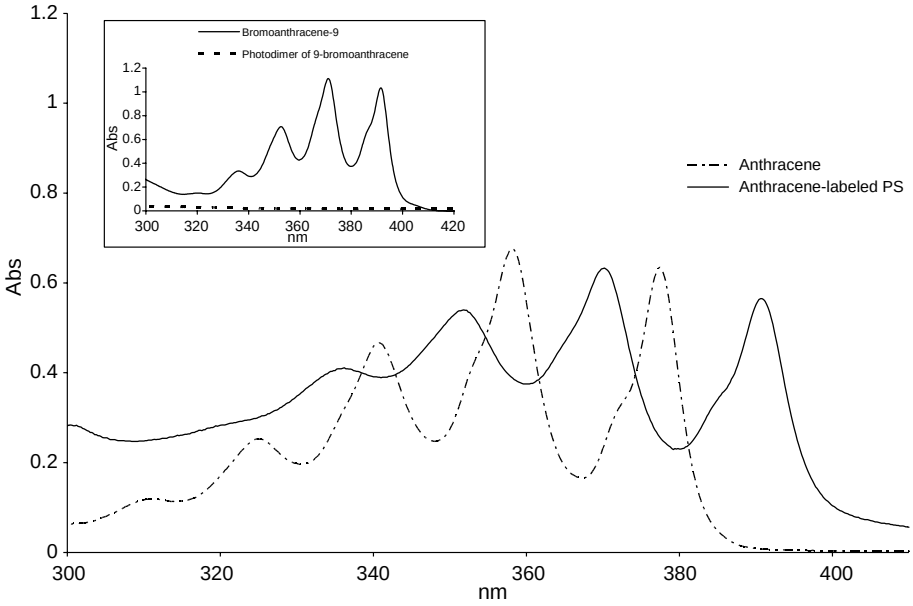

Fig. 5. UV–vis absorbance spectra of THF solutions of anthracene (dashed line, 8.0×10^{-5} M) and anthracene-labeled polystyrene (solid line, 8.0×10^{-5} M, Table 1, run 4). Inset shows UV–vis absrobance spectra of THF solutions of 9-bromoanthracene (solid line, 8.0×10^{-5} M) and the photodimer of 9-bromoanthracene (dashed line, 8.0×10^{-5} M).

temperatures, fewer photodimers of 9-bromoanthracene would be cleaved over the course of the reaction, resulting in polymer chains with lower anthracene content. As shown in Table 3, a correlation between anthracene content and reaction temperature is indeed observed. The reaction performed at 80 °C gave rise to polystyrene with 85% of anthracene labeling (run 1), while lowering the reaction temperature to 60 and 40 °C generated polymers with 35 and 20% anthracene labeling, respectively (runs 2 and 3). Due to the extremely long reaction times required in ATRP reactions of styrene at these low temperatures (96 h for 40 °C) and the possibility of side reactions occurring over such long durations, a monomer that could be polymerized more efficiently at low temperatures was evaluated. As shown in Table 4, when *n*-butyl acrylate, chosen for its increased rate of polymerization compared to styrene [37], was used as the monomer at these lowered temperatures, polymers with PDI values of approximately 1.45 were obtained. Analysis of the reaction mixture using GPC (RI and UV set at 370 nm) indicated no detectable amounts of anthracene absorption in the polymer (Fig. 6, solid trace vs. dashed). Only after amplifying the UV (370 nm) signal by 1.1×10^{4} was an absorbance due to anthracene in the polymer observed. This is consistent with the polymeric product containing largely the centrally- or terminally-bound anthracene photodimers (Scheme 5, e and c), rather than regenerated anthracene end groups (Scheme 5, d).

4. Conclusions

Photodimers of 9-bromoanthracene were studied as initiators in the ATRP of styrene, generating anthracene end-labeled polymers via cleavage of the polymer-bound photodimer during the reaction. Experiments carried out in either the

Table 2
Products obtained in the ATRP of styrene when the addition of 9-bromoanthracene photodimers commenced the polymerization

Run	[M]/[I][a]	[Cu]/[I][b]	$V_{solvent}/V_{total}$	M_n[c] (Da)	PDI M_w/M_n
1	25	1	0.6	11,170	1.53
2	50	2.5	0.7	16,980	1.39
3	50	1	0.6	16,610	1.38
4	100	2.5	0.7	10,740	1.34
5	100	1	0.6	14,000	1.30

Reactions were run for 48 h with PMDETA as the ligand and Cu(I)Cl as the catalyst at 80 °C in THF. The photodimer initiator was added last after the other components was allowed to reach reaction temperature. See Section 2 for details.

[a] Monomer (M) = styrene. Initiator (I) = anthracene photodimer. ([I] = [C–Br sites]).

[b] Catalyst (CuX) to initiating sites (C–Br) ratio. [CuCl]–[PMDETA].

[c] Apparent number average molecular weight compared to PS standards using RI detection.

Table 3
Effect of temperature on the products obtained in the ATRP of styrene using photodimers of 9-bromoanthracene as initiators

Run	Temperature (°C)	Time (h)	M_n[a] (Da)	PDI (M_w/M_n)	Anthracene (%)[b]
1	80	48	26,080	1.75	85
2	60	48	43,100	1.53	35
3	40	96	56,800	1.43	20

Reactions were run in bulk with PMDETA as the ligand, Cu(I)Cl as the catalyst, and [M]:[I] = 50:1 in all cases. Reactions were performed in the dark with [Cu]:[PMDETA]:[C–Br] = 2.5:2.5:1.

[a] Apparent number average molecular weight compared to PS standards using RI detection.

[b] Anthracene was calculated using Beer–Lambert's law from UV–vis data.

Table 4
Results of the ATRP of butyl acrylate using photodimers of 9-bromoanthracene as the initiator

Run	[M]/[I][a]	[Cu]/[I][b]	Temprature (°C)	$V_{Solvent}/V_{Total}$	Time (h)	M_n[c] (Da)	PDI M_w/M_n
1	50	1	60	0.5	48	14,040	1.70
2	50	1	40	0.5	65	11,350	1.43
3	50	1	40	0.5	48	7830	1.47
4	50	1	40	0.5	48	11,870	1.41

Reactions were run in THF with PMDETA as the ligand, Cu(I)Cl as the catalyst. See Section 2 for details.
[a] Monomer (M) = butyl acrylate. Initiator (I) = 9-bromoanthracene photodimer. ([I] = [CBr sites]).
[b] Catalyst (CuX) to initiating sites (C–Br) ratio. [CuCl]–[PMDETA].
[c] Apparent number average molecular weight compared to PS standards using RI detection.

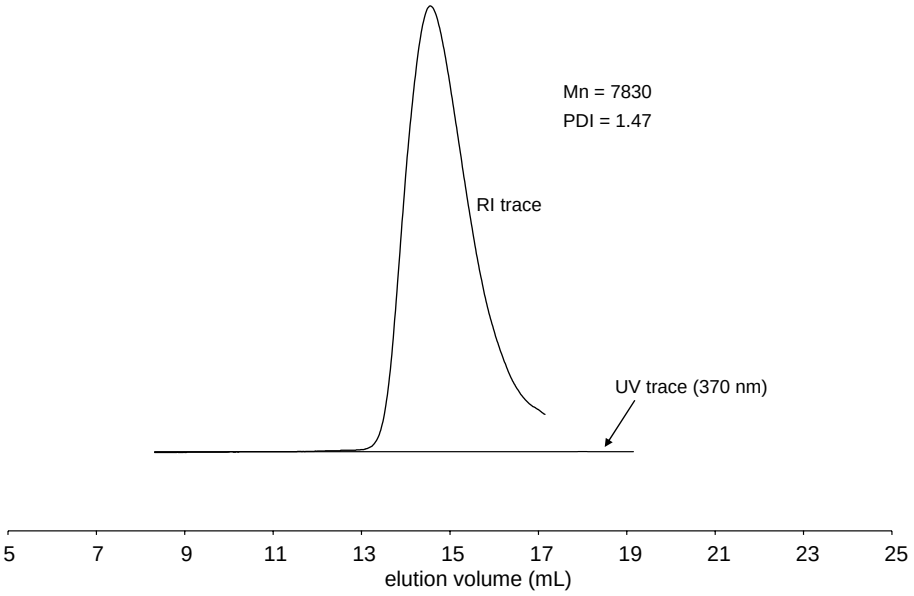

Fig. 6. GPC traces of poly(*n*-butyl acrylate) obtained by ATRP at 40 and 60 °C using photodimers of 9-bromoanthracene as the initiator, Cu(I)Cl as the catalyst, and PMDETA as the ligand (Table 4, run 3). Solid line: RI trace; dashed line: UV trace (370 nm).

presence or absence of light with Cu(I)Br or Cu(I)Cl as the catalyst generated polymers with M_n values 3 to 5-fold higher than anticipated based on monomer to initiating-site ratios, and displayed first order kinetics with respect to monomer concentration at 80 °C. Slow initiation from the bridgehead radical on the initiator, along with continual cleavage of the anthracene photodimer throughout the reaction, appear to be responsible for the relatively high PDI values (>1.4) and non-linear relationship between M_n values and monomer consumption, preventing behavior consistent with a controlled ATRP system. Modifying the order of addition of the reagents, with the initiating photodimer introduced last, reduced heat-induced cleavage prior to initiation, resulted in polymers with lower M_n values and lower PDI values (<1.4). Performing reactions at lower temperatures generated polymers with appreciably less anthracene labeling and lower PDI values, providing additional evidence for the model of heat-induced cleavage of the anthracene photodimer both prior to initiation and during the polymerization. The ability to use aromatic photodimers as ATRP initiators circumvents the need for the synthetic modification often required to produce an initiating site off a chromophoric group.

Acknowledgements

This work was supported by financial contributions from Petroleum Research Fund (Grant No. 39855-GB7), Research Corporation (Grant No. CC6284), Bristol-Myers Squibb, and the Bucknell University Program for Undergraduate Research.

References

[1] Wang J, Matyjaszewski K. Macromolecules 1995;28:7901–10.
[2] Matyjaszewski K, Xia J. Chem Rev 2001;101:2921–90.
[3] Xue L, Agarwal US, Lemstra PJ. Macromolecules 2002;35:8650–2.
[4] De la Fuente JL, Fernandez-Garcia M, Fernandez Sanz M, Madruga EL. J Polym Sci, Part A: Polym Chem 2001;39:3443–50.
[5] Patten TE, Matysjaszewski K. Acc Chem Res 1999;32:895–903.
[6] Matysjaszewski B, Kajiwara A. Macromolecules 1998;31:548–50.
[7] Matysjaszewski K, Patten TE, Xia JH. J Am Chem Soc 1997;119:674–80.
[8] Nanda AK, Matyjaszewski K. Macromolecules 2003;36:599–604.
[9] Gromada J, Matyjaszewski K. Macromolecules 2001;34:7664–71.
[10] Zhang X, Matyjaszewski K. Macromolecules 1999;32:7349–53.
[11] Tong JD, Ni S, Winnik MA. Macromolecules 2000;33:1482–6.
[12] Wang G, Zhu X, Zhenping C, Zhu J. J Polym Sci, Part A: Polym Chem 2005;43:2358–67.
[13] Goodman CC, Roof AC, Tillman ES, Ludwig B, Chon D, Weigley MI. J Polym Sci, Part A: Polym Chem 2005;43:2655–67.

[14] Ohno K, Fujimoto K, Tsujii Y, Fukuda T. Polymer 1999;40:759–63.
[15] Kim CS, Oh SM, Kim S, Cho CG. Macromol Rapid Commun 1998;19: 191–6.
[16] Zhang H, Klumperman B, van der Linde R. Macromolecules 2002;35: 2261–7.
[17] Ohno K, Fujimoto K, Tsujii Y, Fukuda T. Polymer 1999;40:759–63.
[18] Zhang H, Klumperman B, van der Linde R. Macromolecules 2002;35: 2261–7.
[19] Tillman ES, Nossarev GG, Hogen-Esch TE. J Polym Sci, Part A: Polym Chem 2001;39:3121–9.
[20] Tillman ES, Hogen-Esch TE. Macromolecules 2001;34:6616–22.
[21] Coursan M, Desvergne JP. Macromol Chem Phys 1996;197:1599–608.
[22] Goldbach JT, Russell TP, Penelle J. Macromolecules 2002;35:4271–6.
[23] Wolfe JP, Wagnaw S, Macoux J-F, Buchwald SL. Acc Chem Res 1998; 31:805–18.
[24] Okano K, Tokuyama H, Fukuyama T. Org Lett 2003;5:4987–90.
[25] Keegstra MA, Peters THA, Brandsma L. Tetrahedron 1992;48:3633–52.
[26] Klapars A, Huang X, Buchwald SL. J Am Chem Soc 2002;124:7421–8.
[27] Pokorna V, Vyprachticky D, Pecka J, Mikes F. J Fluoresc 1999;9:59–66.
[28] Bouas-Laurent H, Castellan A, Desvergne JP, Lapouyade R. Chem Soc Rev 2000;29:43–55.
[29] Breton GW, Vang X. J Chem Educ 1998;75:81–2.
[30] Pangborn AB, Giardello MA, Grubbs RH, Rosen RK, Timmers FJ. Organometallics 1996;15:1518–20.
[31] Matyjaszewski K, Wang J-L, Grimaud T, Shipp DA. Macromolecules 1998;31:1527–34.
[32] Khoung KS, Jones WH, Pryor WA, Houk KN. J Am Chem Soc 2005;127: 1265–77.
[33] Nanda AK, Matyjaszewski K. Macromolecules 2003;36:8222–4.
[34] Gridnev AA, Ittel SD. Macromolecules 1996;29:5864–74.
[35] Kapfenstein-Doak H, Barner-Kowollik C, Davis TP, Schweer J. Macromolecules 2001;34:2822–9.
[36] $\varepsilon = 10{,}000\ \mathrm{cm}^{-1}\,\mathrm{M}^{-1}$ near 370 nm for anthracene. Anthracene content was calculated using Beer–Lambert's law.
[37] Chambard G, Klumperman B, German AL. Macromolecules 2002;35: 3420–5.